Letter

Extrinsic tunnel Hall effect in MgO-based tunnel junctions

I. Yu. Pashenkin,[1] M. V. Sapozhnikov,[1,2] N. S. Gusev,[1,2] E. A. Karashtin,[1,2] and A. A. Fraerman[1]
[1]*Institute for Physics of Microstructures RAS, Nizhny Novgorod 603950, Russia*
[2]*Lobachevsky State University of Nizhny Novgorod, Nizhny Novgorod 603950, Russia*

(Received 12 May 2022; revised 11 November 2022; accepted 4 December 2022; published 22 December 2022)

The Hall effect that occurs when current flows through a CoFeB/MgO/NM (NM = Pt,Ta) tunnel junction is investigated. It is shown that the transverse voltage in NM electrodes is nonlinear on a DC voltage applied to the tunnel junction. It has both linear (odd) and quadratic (even) parts with respect to electric field. The linear part contains well-known contributions of the anomalous Hall effect in the ferromagnetic electrode, inverse spin-hall effect in NM, and others. The quadratic part is a phenomenon caused by the spin-orbit scattering of electrons in an external electric field induced by a voltage applied to the barrier. This field reaches values of 10^9 V/m, which is close to internal atomic fields. The magnitude of both effects decreases as the thickness of the NM electrode is increased due to shunting effects.

DOI: 10.1103/PhysRevB.106.L220408

Spin-orbit coupling (SOC), which is a relativistic contribution to the interaction between a particle and an electric field, is characterized by the energy

$$H_{\mathrm{SO}} = \lambda \boldsymbol{\sigma} \cdot \mathbf{E} \times \mathbf{p}, \tag{1}$$

which combines the electric field $\mathbf{E}$, particle spin $\boldsymbol{\sigma}$, and momentum $\mathbf{p}$. Despite the fact that it is a relativistic interaction, the effects associated with it appear in a significant way especially in the solid states where SOC is enhanced by a factor of about m_0c^2/E_G, where $E_G \sim 1$ eV is the gap [1,2]. There the spin-orbit effects are mainly caused by the motion of electrons, which act as charge and spin carriers, and the electric field of atomic nuclei. That is why SOC is strongest in metals with a large atomic weight, such as Pt, Ta, W, and Bi. SOC can affect both localized electrons and conduction electrons. In the first case it leads to well-known phenomena of magnetic anisotropy. In the case of electron transport, SOC results in the spin Hall effect (SHE) [3]. The effect consists of the appearance of spin accumulations on the lateral surfaces of an electric current-carrying sample. It was originally predicted by Dyakonov and Perel in 1974 [4,5] and then discovered experimentally in 2004 [6]. The inverse SHE (ISHE) is observed when a pure spin current (or a spin-polarized electric current) flows in a material with a strong SOC. This leads to the appearance of a transverse charge current (or to charge accumulation on the lateral surfaces) [7,8]. A particular example of ISHE is the anomalous Hall effect (AHE) since the electric current in magnetic materials is initially spin polarized due to the internal exchange splitting.

SHE and ISHE has now become the basis of a rapidly developing new branch of condensed state physics-spin orbitronics [9]. It is believed that a possibility of mutual conversion of electric and spin currents will open the prospect for energy-efficient logic and memory devices for information processing [9–13].

In transition metals such as Co or Fe, which are used as spin-polarized current injectors, the degree of spin polarization of electrons is about 60% [14]. The use of a tunnel magnetic junction with a MgO dielectric layer together with CoFeB ferromagnet as an injector makes it possible to increase the spin polarization to almost 100% [15]. So SHE in the systems with tunnel barrier was also studied recently [16–20]. In this regard, a question arises about the possible effects of SOC directly in the tunnel gap. Scattering by magnetic impurities in the barrier and a frozen-in boundary electric field are considered in [21–23], respectively. In all the above examples the electric field causing SOC according to (1) is the internal atomic field. In [24], the authors considered theoretically the problem of the SOC with the external field applied to the tunnel barrier and showed the possibility of a transverse (Hall) current in the system. Below we will refer to the Hall effect caused by any SOC mechanism in the tunnel gap as the tunnel Hall effect (THE).

In our work we experimentally study the THE in a CoFeB/MgO/NM (NM = Pt,Ta) tunnel junctions. The idea is that the strong electric field in the gap can lead not only to linear, but also to nonlinear effects. Phenomenologically, based on symmetry considerations, the easiest expression for the effective transverse electric field causing Hall voltage can be written as

$$\mathbf{E}_{\mathrm{Hall}} = \alpha[\mathbf{j} \times \mathbf{M}] + \beta[\mathbf{n} \times \mathbf{M}](\mathbf{jE}). \tag{2}$$

Here $\mathbf{M}$ is magnetization, $\mathbf{E}$ is applied external electric field, $\mathbf{j} = \sigma\mathbf{E}$ is the transport current, and α and β are phenomenological constants. $\mathbf{n}$ is a vector characterizing the nonreciprocity of the system; in the case under consideration it is the normal to the interface between the layers. The first term in (2) is the linear Hall effects of a different nature such as AHE, SHE, or intrinsic THE caused by asymmetry of the tunnel barrier. They are caused by the SOC of the tunneling electron with the internal atomic electric fields. All

these effects are proportional to the applied electric field, which determines only the magnitude of the flowing current j in accordance with Ohms law. Therefore $U_{\text{Hall}} \sim j \sim E$. The second term is quadratic according to the external electric field since it enters the expression not only through the transport current, but also directly, $U_{\text{Hall}} \sim jE \sim E^2$. Formally, the second term looks as if the interaction of the transport current with an external electric field leads to a transverse current. One of the obvious possible physical reasons behind the possible nonlinear effect is the SOC of tunneling electrons with an external field. Indeed, the magnitude of the field in the tunnel gap can be as large as 10^9 V/m, which approaches the magnitude of the internal atomic fields and should lead to the appearance of a transverse current in the system. To distinguish this effect from other linear Hall effects in the system, which are caused by internal atomic electric fields, we hereafter refer to this effect as an extrinsic tunnel Hall effect (eTHE) as it caused by external field. Expression (2) may also contain terms of higher orders in M, as well as terms containing spatial derivatives of M that are also proportional to the product of the current and the external field. They will correspond to other microscopic mechanisms, but in any case, these will be effects associated with the SOC of tunneling electrons (j) and a strong electric field in the barrier (E). A detailed discussion of the possible specific microscopic mechanisms of SOC in the tunnel barrier is beyond the scope of our experimental work and should be the result of further research. Regardless of the specific microscopic mechanism an important obvious feature of such eTHE should be its quadratic dependence on the applied electric field.

The studied structures Ta(20)/CoFeB(10)/MgO(1.5)/Pt(t) and Ta(20)/CoFeB(10)/MgO(1.5)/Ta(2) (thicknesses are given in nm) are deposited on $Si/SiO_2/Si_3N_4$ substrates by magnetron sputtering. The base pressure in the chamber does not exceed 10^{-7} Torr. To make measurements of the tunneling Hall effect, the top Pt(Ta) and MgO layers are patterned by optical lithography and ion etching into a micron-sized T-shape, as shown in Fig. 1. The area of the top NM-electrode is about 60 μm^2. The bottom CoFeB electrode has a rectangular shape of 20 × 1000 μm. It is deposited in an in-plane external magnetic field (∼200 Oe) to induce easy axis anisotropy along the long side of the electrode. The resistance-area product of the tunnel junction is about 15 kΩ × μm^2. To increase the spin polarization of the tunneling electrons, the samples are annealed in vacuum at 330° C for 2 hours. The magnetic tunnel junctions CoFeB/MgO/CoFeB fabricated by us using a similar technology as a reference, demonstrates an increase in the tunnel magnetoresistive effect from 10% to 200% due to thermal annealing. This corresponds to an increase of the spin polarization of the current in the structure from 30 to 70% according to the Julier formula [25]. This is due to the crystallization of the initially amorphous CoFeB into the bcc (001) texture from the boundary with MgO (001) [26]. The specific crystal structure is essential for the coherent tunneling process and observation of the so-called giant tunnel magnetoresistive effect [27], which indicates a high spin polarization of current in the structure. The same high spin polarization in the CoFeB/MgO/NM structure is important because the observed Hall effects directly depend on the spin polarization of tunneling electrons. The thicknesses of the top Pt electrode

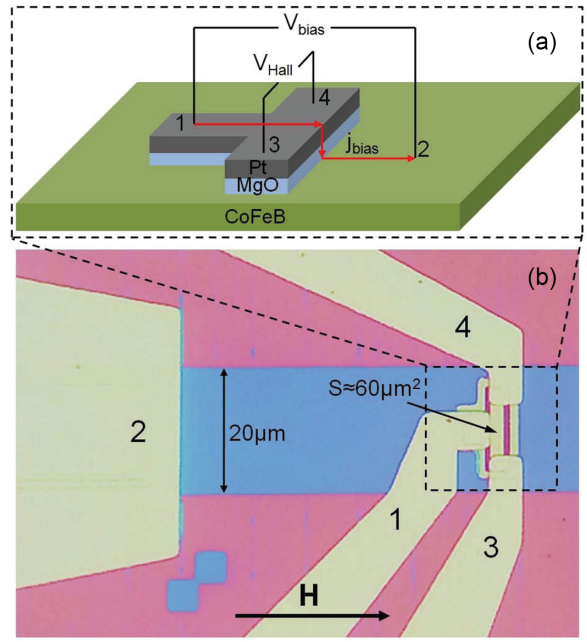

FIG. 1. (a) Geometry of the sample and measurements. (b) Optical microscope image of the sample. Numbers of the electrodes correspond to the scheme (a). "S" denotes the area of the tunnel junction, the arrow indicates the direction of applied magnetic field.

are 1, 2, and 10 nm for different samples. The thickness of the Ta top electrode is 2 nm. In the case of the tunnel Hall effect the Hall current in the normal metal layer flows in the subsurface region not exceeding the momentum relaxation length of tunneling electrons, which is several nanometers [28]. The current caused by the inverse spin Hall effect is induced on the spin relaxation length, which varies in the range from 1 to 10 nm according to the literature [29]. We further show that this length is between 2 nm and 10 nm from our measurements. Therefore, the top NM-electrode must be ultra-thin to eliminate the shunting effect and thereby increase the signal-to-noise ratio.

Transport measurements are carried out in the inverse spin Hall effect geometry. A DC bias voltage is applied to leads 1 and 2 ($V_{\text{bias}} = V_{12}$) and the Hall signal is measured between leads 3 and 4 depending on the external magnetic field applied in the plane of the film, as shown in Fig. 1. The magnetization of the CoFeB electrode is aligned along the easy-axis direction defined by the deposition process and can be switched with an external magnetic field **H** (Fig. 1). The Hall effects are measured by applying a bias current from the CoFeB injector into the Pt collector or in the opposite direction. The current is spin polarized according to CoFeB magnetization.

The measured voltage signal V_{34} contains both Hall voltage and an additional contribution of magnetoresistance due to asymmetry of the geometric shape of the sample. The Hall effects are odd with respect to the applied magnetic field, while the effects due to the magnetoresistance are even. This makes it possible to extract the Hall effects from the measured signal as an odd part of $V(\mathbf{H})$ (see Supplemental Material for the details [30]). Below in the text, always under the Hall signal, Hall voltage, and so on the part of the initially measured

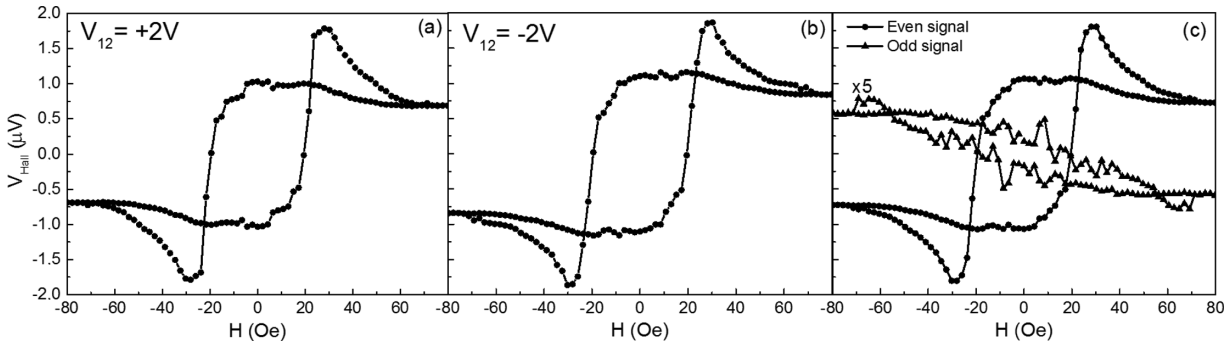

FIG. 2. Typical magnetic field dependencies of the Hall voltage for (a) positive and (b) negative DC bias voltage $V_{\text{bias}} = \pm 2$ V applied to tunnel barrier. The thickness of the top Pt electrode is 1 nm. (c) Sum (solid line) and difference (dashed line) of (a), (b) Hall voltage curves which correspond to even and odd parts with respect to electric field of initial Hall signal, respectively. The graphs shown are the result of averaging the 70 measurements taken.

transverse signal that is odd with respect to magnetic field is implied. All subsequent discussions about the parity and oddness of the Hall signal itself will refer to its dependence on the electric field applied to the contact.

The Hall voltage measurements are carried out at different values and both polarities of the DC voltage applied to the tunnel barrier. Figures 2(a) and 2(b) show the typical Hall voltage hysteresis. The thickness of the top Pt electrode in this case is 1 nm. The initial signals contain contributions from both the tunnel Hall effect and the anomalous and inverse spin Hall effect. A change in the polarity of the voltage applied to the tunnel contact does not lead to a change in the sign of the measured effect, however, the amplitude of the signal changes. Thus, the signal can be divided into an odd part with respect to electric field in the V_{bias} part which depends on the polarity of V_{bias} and an even part which does not depend on the polarity of the V_{bias}, but depends only on its magnitude

$$V_{\text{Hall}}^{\text{odd}} = \{V_{\text{Hall}}(H, +V_{\text{bias}}) - V_{\text{Hall}}(H, -V_{\text{bias}})\}/2,$$
$$V_{\text{Hall}}^{even} = \{V_{\text{Hall}}(H, +V_{\text{bias}}) + V_{\text{Hall}}(H, -V_{\text{bias}})\}/2. \quad (3)$$

Both of them are presented in Fig. 2(c).

Figure 3 shows the $V_{\text{Hall}}(\mathbf{H})$ curves at different values of the voltage V_{bias} applied to the tunnel barrier. The value of the voltage applied directly to the tunnel barrier itself is actually lower than the values of V_{bias} indicated on the graphs because the resistance of the supply electrodes is approximately two-thirds of the total resistance R_{12}. This is established by measuring short-circuit tunnel barriers. It can be seen that an even Hall signal increases nonlinearly on the applied electric field [Fig. 3(a), which is not observed for an odd signal [Fig. 3(b). The graphs show the data for the effect, linear in the electric field, only for $V_{\text{bias}} \leqslant 2$V. This is due to the fact that as the V_{bias} increases, the value of the linear contribution becomes small at the background of the nonlinear part, and as a result, the signal-to-noise ratio decreases for it, which can be seen in Fig. 3(b). For each sample, measurements are made with a gradual increase in V_{bias} until an electrical breakdown is observed ($4 - 5$ V for different samples).

A control measurement of the Hall signal made for a sample in a magnetic field oriented in the transverse direction (i.e., directed along the Hall contacts) with $H = 150$ Oe, $V_{\text{bias}} = 4$ V gives $V_{\text{Hall}} = 1 \pm 1\mu$ V. A small possibly nonzero signal in this case can be explained by insufficient accuracy of the geometry of the sample and measurement scheme.

The dependence of an even Hall signal amplitude on V_{bias} measured in a saturation magnetic field is approximated accurately by a parabola (Fig. 4). The odd Hall signal is well approximated by a line and probably corresponds to the anomalous and inverse spin Hall effects. So

$$V_{\text{Hall}} = V_{\text{Hall}}^{\text{odd}} + V_{\text{Hall}}^{\text{even}} = \alpha V_{\text{bias}} + \beta V_{\text{bias}}^2, \quad (4)$$

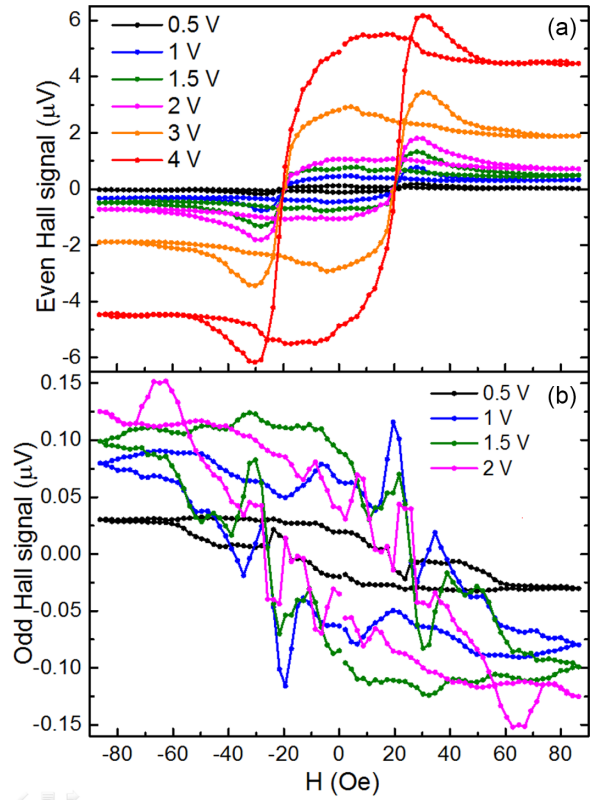

FIG. 3. Even with respect to electric field (a) $V_{\text{Hall}}^{\text{even}}$ and (b) odd $V_{\text{Hall}}^{\text{odd}}$ part of $V_{\text{Hall}}(H)$ curves for different values of the applied bias voltage. Thickness of the top Pt electrode is 1 nm. The graphs shown are the result of averaging $50 - 150$ measurements taken.

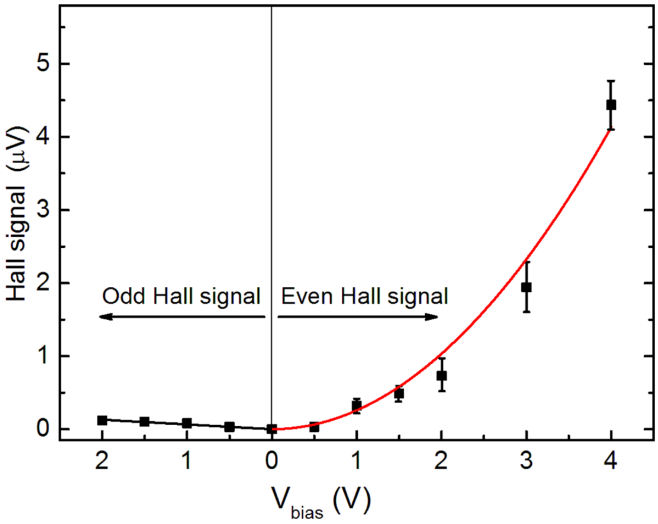

FIG. 4. Voltage dependence of the even part with respect to electric field (right side) and the odd (left side) part of initial Hall signal in the sample with 1-nm Pt electrode measured in saturation. The even part is well approximated by a parabola and the odd part approximated by a line.

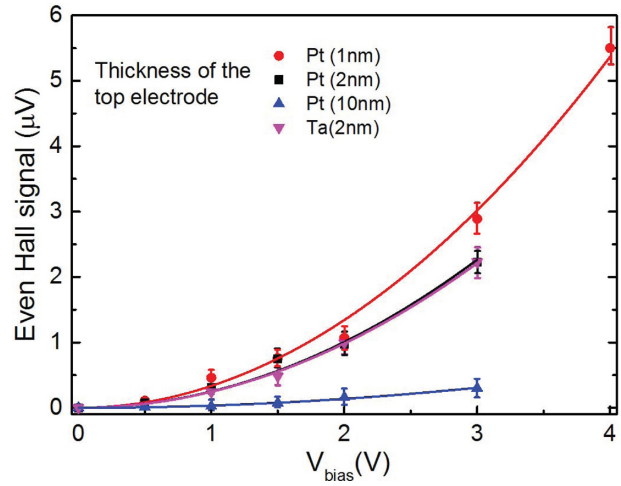

FIG. 5. Voltage dependence of an even part of the Hall signal at the zero external magnetic field. Evidently the curves for the samples with 2-nm Pt and 2-nm Ta top electrodes practically coincides.

where α and β are constants determined from our experiment. The quadratic part represents the sought-for manifestation of the spin-orbit effect associated with a strong external electric field applied to the tunnel gap. The odd part includes all other possible Hall effects, which are linearly proportional to applied voltage, such as an anomalous effect in a magnetic electrode or an inverse spin-hall effect in a platinum electrode. Evidently, they should change sign with the inversion of electric current. The observed nonlinear effect cannot be explained by the possible nonlinearity of the current-voltage characteristic of the system since it does not change sign when the sign of the voltage applied to the system changes [compare Figs. 2(a) and 2(b)]. Nonlinear effects associated with the nonlinearity of the current-voltage characteristic would have to change sign when the direction of the applied current changes.

Note that when current flows through the tunnel barrier, a temperature gradient can occur. It can lead to a nonlinear Hall effect, proportional to the current caused by this gradient as the additional current appears $j_{\Delta T} \sim \Delta T \sim E^2$ (ΔT is the temperature difference across the barrier), which contributes to the first term in (2). Nevertheless, this $j\Delta T$ is incommensurably less than conduction current caused by the applied voltage, as for sure $k_B\Delta T \ll 1$ eV. So the even effects caused by the temperature gradients should be much less than the linear effects caused by conductive current. On the contrary, the nonlinear effect observed by us significantly exceeds the linear effect in magnitude and therefore cannot be explained by temperature gradients.

Although the calculation of the phenomenological coefficients α and β is based on measurements made in a saturating field to have a uniform magnetic state of the sample, similar quadratic dependences are observed for the magnitude of the Hall effect in the remanent magnetic state (Fig. 5). An increase in the thickness of the top Pt electrode, as expected, leads to a decrease in the Hall voltage and particularly in an even part of initial signal. The data for α and β coefficient are presented in Table I. Although the values of α and β coefficients noticeably decrease with the increasing thickness of Pt, the general character of dependence (4) is retained.

Measurements of the sample with the 2-nm Ta top electrode show the similar nonlinear Hall effect. Besides its magnitude (characterized by value of the β coefficient) is practically the same as in the sample with the Pt top electrode of the same thickness (see Table I). Whereas the α coefficient is three times smaller and has different sign. Since the SOC constants in Ta and Pt differ by an order of magnitude [31], the observed quadratic effect cannot be due to spin-Hall scattering in the upper NM electrode.

The linear part of V_{Hall} determined by α allows us to estimate the overall spin Hall angle θ_{SH} in the investigated system. Let us estimate its value for the Pt as an example. We suppose that the thickness of the Pt layer $t = 1$ nm is much less than the spin relaxation length, which seems to be several nanometers according to our measurements (the Hall voltage is slightly smaller for $t = 2$ nm than for $t = 1$ nm and is still observable for $t = 10$ nm). Then using the definition of the spin Hall angle and simple geometric relations we have

$$\theta_{SH} = \frac{1}{P_s}\frac{j_{\text{Hall}}^{\text{linear}}}{j_{\text{bias}}} = \frac{1}{P_s}\frac{RS}{\rho w}\alpha \approx 0.007, \tag{5}$$

where R is the sample resistance (1 kΩ), ρ is the resistivity of platinum electrode ($1.07 \times 10^{-7}\Omega \times$ m), w is the distance between electrodes 3 and 4 (8 μm; see Fig. 1), S is the tunnel

TABLE I. The data for α and β coefficients for different Pt electrode thickness.

d (nm)	α	β (V^{-1})
$Pt(1)$	$6.5 \times 10^{-8} \pm 0.3 \times 10^{-8}$	$3.4 \times 10^{-7} \pm 0.07 \times 10^{-7}$
$Pt(2)$	$8 \times 10^{-8} \pm 10^{-8}$	$2.6 \times 10^{-7} \pm 0.4 \times 10^{-7}$
$Pt(10)$	$0.6 \times 10^{-8} \pm 10^{-8}$	$0.3 \times 10^{-7} \pm 0.04 \times 10^{-7}$
$Ta(2)$	$-3 \times 10^{-8} \pm 3 \times 10^{-8}$	$2.5 \times 10^{-7} \pm 0.12 \times 10^{-7}$

contact square (60 μm^2), and P_s is the spin polarization of the current (70%, determined from the data for a reference CoFeB/MgO/CoFeB sample). The spin Hall angle for platinum varies in the range from 0.0067 to 0.027 or even greater, according to the literature [29,32,33]. Thus we obtain the estimation for our sample which corresponds to the literature by the order of value. In addition to this inverse spin Hall effect, we observe a Hall effect caused by spin-orbit scattering of electrons inside the barrier which is an order of magnitude greater at higher applied voltages.

It is also possible to estimate the spin-orbit constant λ in (1) from our measurements. Using a simple estimation in the limit of small electron tunneling probability we obtain (see Supplemental Material for details [30])

$$\lambda \sim \frac{j_{\mathrm{Hall}}}{j_{\mathrm{bias}}} \frac{L v_f}{2 P_s V_{\mathrm{bias}}} \sim 2 \times 10^{-5} \frac{A s^2}{k g}, \tag{6}$$

where L is the tunneling barrier thickness, v_f is the Fermi velocity, which gives the same result as the calculation [22] by the order of value. The estimated constant of spin-orbit coupling is much greater than that constant in a vacuum [1,2], which leads to an observable Hall effect.

In conclusion, we investigated the transverse transport effect that occurs when spin-polarized electrons tunnel through the tunnel barrier in CoFeB/MgO/(Pt,Ta) junction. We experimentally found the Hall effect due to spin-orbit coupling of tunneling electrons with a high external electric field applied to the barrier. The tunnel Hall voltage on NM electrodes depends quadratically on the DC voltage applied to the barrier. This means that it is possible to control and manipulate the spin-orbit scattering of spin-polarized electrons in the barrier by voltage.

This research was supported by the Russian Science Foundation (Grant No. 21-12-00271).

[1] E. I. Rashba, Spin-orbit coupling and spin transport, Phys. E **34**, 31 (2006).
[2] L. Petersen and P. Hedegard, A simple tight-binding model of spin-orbit splitting of sp-derived surface states, Surf. Sci. **459**, 49 (2000).
[3] J. Sinova, S. O. Valenzuela, J. Wunderlich, C. H. Back, and T. Jungwirth, Spin Hall effects, Rev. Mod. Phys. **87**, 1213 (2015).
[4] M. I. Dyakonov and V. I. Perel, Possibility of orientating electron spins with current, JETP Lett. **13**, 467 (1971).
[5] M. I. Dyakonov and V. I. Perel, Current-induced spin orientation of electrons in semiconductors, Phys. Lett. A **35**, 459 (1971).
[6] Y. Kato, R. C. Myers, A. C. Gossard, and D. D. Awschalom, Observation of the Spin Hall Effect in Semiconductors, Science **306**, 1910 (2004).
[7] N. S. Averkiev and M. I. Dyakonov, Current due to nonhomogeneous spin orientation in semiconductors, JETP Lett. **35**, 196 (1983).
[8] A. A. Bakun, B. P. Zakharchenya, A. A. Rogachev, M. N. Tkachuk, and V. G. Fleisher, Detection of a surface photocurrent due to electron optical orientation in a semiconductor, JETP Lett. **40**, 1293 (1984).
[9] L. Liu, C.-F. Pai, Y. Li, H. W. Tseng, D. C. Ralph, and R. A. Buhrman, Spin-torque switching with the giant spin Hall effect of tantalum, Science **336**, 555 (2012).
[10] T. Kuschel and G. Reiss, Charges ride the spin wave, Nat. Nanotechnol. **10**, 22 (2015).
[11] A. Manchon, J. Železný, I. M. Miron, T. Jungwirth, J. Sinova, A. Thiaville, K. Garello, and P. Gambardella, Current-induced spin-orbit torques in ferromagnetic and antiferromagnetic systems, Rev. Mod. Phys. **91**, 035004 (2019).
[12] S. Manipatruni, D. E. Nikonov, C.-C. Lin, T. A. Gosavi, H. Liu, B. Prasad, Y.-L. Huang, E. Bonturim, R. Ramesh, and I. A. Young, Scalable energy-efficient magnetoelectric spin-orbit logic, Nature (London) **565**, 35 (2019).
[13] P. A. Dowben, D. E. Nikonov, A. Marshall, and Ch. Binek, Magneto-electric antiferromagnetic spin-orbit logic devices, Appl. Phys. Lett. **116**, 080502 (2020).
[14] R. Meservey and P. M. Tedrow, Spin-polarized electron tunneling, Phys. Rep. **238**, 173 (1994).
[15] X.-G. Zhang and W. H. Butler, Large magnetoresistance in bcc Co/MgO/Co and FeCo/MgO/FeCo tunnel junctions, Phys. Rev. B **70**, 172407 (2004).
[16] L. Liu, C.-T. Chen, and J. Z. Sun, Spin Hall effect tunnelling spectroscopy, Nat. Phys. **10**, 561 (2014).
[17] L. Liu, A. Richardella, I. Garate, Y. Zhu, N. Samarth, and C.-T. Chen, Spin-polarized tunneling study of spin-momentum locking in topological insulators, Phys. Rev. B **91**, 235437 (2015).
[18] C. Fang, C. H. Wan, B. S. Yang, J. Y. Qin, B. S. Tao, H. Wu, X. Zhang, X. F. Han, A. Hoffmann, X. M. Liu, and Z. M. Jin, Determination of spin relaxation times in heavy metals via second-harmonic spin injection magnetoresistance, Phys. Rev. B **96**, 134421 (2017).
[19] K. Nakagawara, S. Kasai, J. Ryu, S. Mitani, L. Liu, M. Kohda, and J. Nitta, Temperature-dependent spin Hall effect tunneling spectroscopy in platinum, Appl. Phys. Lett. **115**, 162403 (2019).
[20] M. Götte and T. Dahm, Determination of Out-of-Plane Spin Polarization of Topological Surface States by Spin Hall Effect Tunneling Spectroscopy, Phys. Status Solidi B **258**, 2000032 (2021).
[21] A. Vedyayev, N. Ryzhanova, N. Strelkov, and B. Dieny, Spontaneous Anomalous and Spin Hall Effects Due to Spin-Orbit Scattering of Evanescent Wave Functions in Magnetic Tunnel Junctions, Phys. Rev. Lett. **110**, 247204 (2013).
[22] S. A. Tarasenko, V. I. Perel, and I. N. Yassievich, In-Plane Electric Current Is Induced by Tunneling of Spin-Polarized Carriers, Phys. Rev. Lett. **93**, 056601 (2004).
[23] A. Matos-Abiague and J. Fabian, Tunneling Anomalous and Spin Hall Effects, Phys. Rev. Lett. **115**, 056602 (2015).
[24] A. V. Vedyayev, M. S. Titova, N. V. Ryzhanova, M. Ye. Zhuravlev, and E. Y. Tsymbal, Anomalous and spin Hall effects in a magnetic tunnel junction with Rashba spin-orbit coupling, Appl. Phys. Lett. **103**, 032406 (2013).
[25] M. Julliere, Tunneling between ferromagnetic films, Phys. Lett. A **54**, 225 (1975).

[26] Y. Lu, C. Deranlot, A. Vaurés, F. Petroff, and J.-M. George, Effects of a thin Mg layer on the structural and magnetoresistance properties of CoFeB/MgO/CoFeB magnetic tunnel junctions, Appl. Phys. Lett. **91**, 222504 (2007).

[27] S. Yuasa and D. D. Djayaprawira, Giant tunnel magnetoresistance in magnetic tunnel junctions with a crystalline MgO(001) barrier, J. Phys. D: Appl. Phys. **40**, R337 (2007).

[28] D. Gall, Electron mean free path in elemental materials, J. Appl. Phys. **119**, 085101 (2016).

[29] V. Vlaminck, J. E. Pearson, S. D. Bader, and A. Hoffmann, Dependence of spin-pumping spin Hall effect measurements on layer thicknesses and stacking order, Phys. Rev. B **88**, 064414 (2013).

[30] See Supplemental Material at http://link.aps.org/supplemental/10.1103/PhysRevB.106.L220408 for more details.

[31] C. Bull, S. M. Hewett, R. Ji, C.-H. Lin, T. Thomson, D. M. Graham, and P. W. Nutter, Spintronic terahertz emitters: Status and prospects from a materials perspective, APL Mater. **9**, 090701 (2021).

[32] O. Mosendz, V. Vlaminck, J. E. Pearson, F. Y. Fradin, G. E. W. Bauer, S. D. Bader, and A. Hoffmann, Detection and quantification of inverse spin Hall effect from spin pumping in permalloy/normal metal bilayers, Phys. Rev. B **82**, 214403 (2010).

[33] O. Mosendz, J. E. Pearson, F. Y. Fradin, G. E. W. Bauer, S. D. Bader, and A. Hoffmann, Quantifying Spin Hall Angles from Spin Pumping: Experiments and Theory, Phys. Rev. Lett. **104**, 046601 (2010).